PHOTONUCLEAR REACTIONS

E. Oset

Departamento de Física Teórica and IFIC,
Centro Mixto Universidad de Valencia-CSIC,
46100 Burjassot (Valencia) Spain.

Abstract

A successful many body approach to evaluate inclusive photonuclear cross sections is reviewed. The lectures begin with an exposition of the state of the art in the elementary reactions $\gamma N \to \pi N$ and $\gamma N \to \pi\pi N$, which are the basic building blocks for the many body theory. Through the skilful use of Field Theoretical Techniques one can disentangle the different reaction channels in the total photonuclear cross section. The method makes use of genuine reaction probabilities, defined as one step processes and calculated microscopically, and a Monte Carlo simulation procedure by means of which one generates all possible multistep processes which occur in the actual physical reactions. This allows one to compare directly the theoretical results with the experimental cross sections like $(\gamma, \pi), (\gamma, N), (\gamma, NN), (\gamma, N\pi)$ etc. in nuclei.

Index

1 Introduction.

Because of the relative small strength of the electromagnetic interaction and its adequate knowledge from the theoretical point of view, electrons and photons have been taditionally excellent probes of nuclear structure and continue to be so. With increasing experimental hability to perform high resolution as well as coincidence experiments, the wealth of experimental information has reached a point which allows one to learn about details of nuclear structure as well as to dig into the complicated or subtle excitation mechanisms of the nucleus. One theoretical approach which has proved particularly rewarding to put in a unified framework all the different photonuclear reactions is the one based on a many body approach to the general problem using Quantum Field Theoretical Techniques, which allows the separation of all the reaction channels in the (e, e') or γ-nucleus interaction and which we will expose here. For this purpose we shall begin with the study of the $\gamma N \rightarrow \pi N$ and $\gamma N \rightarrow \pi\pi N$ reactions. Then they serve as the starting point in a many body theory which generates two and three nucleon mechanisms for the γ nuclear interaction. A skilful classification of the diagrams allows the separation of genuine one step mechanisms, where all meson correlating two nucleons are off shell, from those diagrams where some intermediate meson is mostly on shell and which can be better dealt with by associating the mechanism to a two step process. These two step and multistep processes are considered by means of a Monte Carlo simulation procedure on which one has a certain control and which requires as input only the probabilities associated to the genuine one step procecess (involving one or many nucleons). With this procedure one can evaluate cross sections for all the channels of the inclusive $\gamma - A$ reaction, $(\gamma, \pi), (\gamma, N), (\gamma, 2N), (\gamma, N\pi)$ etc.

A general good agreement with experiment in all the channels is reached. The method allows the investigation of channels so far unmeasured which contain very much information on magnitudes like the pion absorption probabilities or the nucleon mean free path in the nucleus.

2 The $\gamma N \rightarrow \pi N$ reaction.

From the very beginning we will disregard processes involving $\gamma N \rightarrow \gamma N$ which are of order e^2 in the amplitude and hence we shall start from the photoproduction amplitude $\gamma N \rightarrow \pi N$, and associated amplitudes, which are of order e in the amplitude.

We shall illustrate the model of ref. [1] which follows closely the one introduced in [2]. The model contains the nucleon and delta pole terms, plus their crossed terms, the pion pole and the Kroll Ruderman terms, as shown in fig. 1.
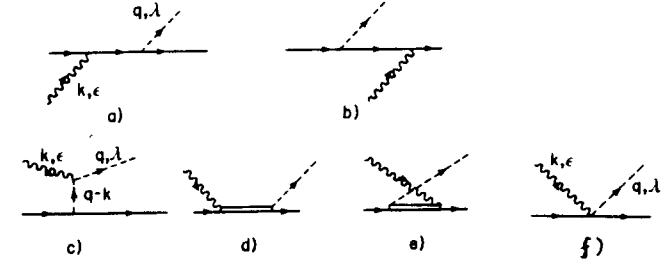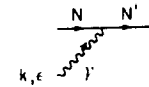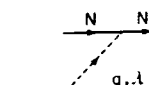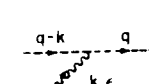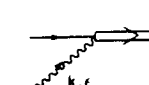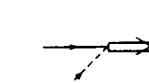

Fig. 1: Feynman diagrams considered for the $\gamma N \rightarrow \pi N$ process. (a) Nucleon pole. (b) Crossed nucleon pole. (c) Pion pole. (d) Delta pole. (e) Crossed delta pole. (f) Kroll Ruderman term.

The amplitudes for these diagrams can be easily obtained from standard Feynman rules using the basic vertices which we detail below

$$-i\delta\tilde{H}_{\gamma NN} = -ie\left(\gamma^\mu + i\frac{\chi_P}{2M}\sigma^{\mu\nu}k_\nu\right)\varepsilon_\mu,$$

$$-i\delta\tilde{H}_{\pi NN} = \frac{f}{\mu}\boldsymbol{\sigma} \cdot \mathbf{q}\tau^\cdot$$

$$-i\delta\tilde{H}_{\gamma\pi\pi} = \mp ie\,(2q - k)^\mu \varepsilon_\mu = \pm ie2q\varepsilon\,,$$

$$-i\delta\tilde{H}_{\gamma N\Delta} = -\frac{f_\gamma}{\mu}(\mathbf{S}^\cdot \times \mathbf{k}) \cdot \boldsymbol{\varepsilon}\,T_\lambda^\cdot + \text{h.c.}\,,$$

$$-i\delta\tilde{H}_{\pi N\Delta} = \frac{f^*}{\mu}(\mathbf{S}^\cdot \cdot \mathbf{q})T_\lambda^\cdot + \text{h.c.}\,,$$

The Kroll Ruderman term is generated from the pseudovector πNN Lagrangian,

$$\delta\mathcal{L}_{\pi NN} = -\frac{g}{2M}\bar{\Psi}\gamma^\mu\gamma_5\vec{\tau}\Psi\partial^\mu\Phi \tag{1}$$

by minimal coupling, $\partial_\mu \rightarrow \partial_\mu + ieA_\mu$. However, it is customary to separate the

nucleon propagator into the positive and negative energy state contributions, as done in eq. (2) and include the contribution of the nucleon direct and crossed terms with negative energy states in the Kroll Ruderman term.

$$\frac{\not{p}+M}{p^2-M^2+i\epsilon}=\frac{M}{E(p)}\left(\frac{\sum_r u(p,r)\bar{u}(p,r)}{p^0-E(p)+i\epsilon}+\frac{\sum_r v(-p,r)\bar{v}(-p,r)}{p^0+E(p)-i\epsilon}\right),$$

(2)

Then only the positive energy intermediate states are considered in the nucleon pole term and the Kroll Ruderman term becomes

$$-iT_\alpha = e\frac{f}{\mu}C(\alpha)\boldsymbol{\sigma}\cdot\boldsymbol{\varepsilon},$$

(3)

with $C(\alpha)$ given by

$$C(\alpha)=\begin{cases} \sqrt{2}\left(1-\frac{\omega(q)}{\sqrt{s}+M}\right) & \text{for } \gamma p \to \pi^+ n \\[2mm] -\sqrt{2}\left(1+\frac{\omega(q)}{E(k)-\omega(q)+E(k+q)}\right) & \text{for } \gamma n \to \pi^- p \\[2mm] -\omega(q)\left(\frac{1}{\sqrt{s}+M}+\frac{1}{E(k)-\omega(q)+E(k+q)}\right) & \text{for } \gamma p \to \pi^0 p \\[2mm] 0 & \text{for } \gamma n \to \pi^0 n \end{cases}$$

(4)

in agreement up to $0(k/M)$ terms with the results obtained from current algebra and PCAC [3]

In the vertices of the Feynman rules M is the nucleon mass, μ the pion mass, $f = 1$, $f_\gamma = 0.12$, $\vec{\sigma}$ the nucleon spin, $\vec{q},\vec{k}$ the pion and photon momenta and ε^μ the photon polarization vector. We work usually in the Coulomb gauge, $\varepsilon^0 = 0$, $\vec{\varepsilon}.\vec{k} = 0$.

In the vertex γNN, χ_p is the proton anomalous magnetic moment. For the coupling of the photon to the neutron the γ^μ term does not appear and χ_p is replaced by χ_n, the neutron anomalous magnetic moment. $E(p)$, $\omega(q)$ are the relativistic energies of the nucleon and the pion and s in eqs. (4) the πN Mandelstam variable.

The operators $\vec{S},\vec{T}$ appearing in the $\pi N\Delta$ and $\gamma N\Delta$ vertices are the spin and isospin transition operators from 1/2 to 3/2.

The model exposed is not exactly unitary and different prescriptions are taken to unitarize it and force it to satisfy Watson's theorem. The practical changes are small. In [1] the method of Olson [4] is used to implement unitarity

in the model by multiplying the delta pole term by a small phase such that the $\gamma N \to \pi N$ amplitude has the same phase as the $\pi N \to \pi N$ scattering amplitude in every partial wave and isospin channel (Watson's theorem). The agreement of the model with experiment is generally good as can be seen in fig. [1] where we show two examples of cross sections obtained with this model
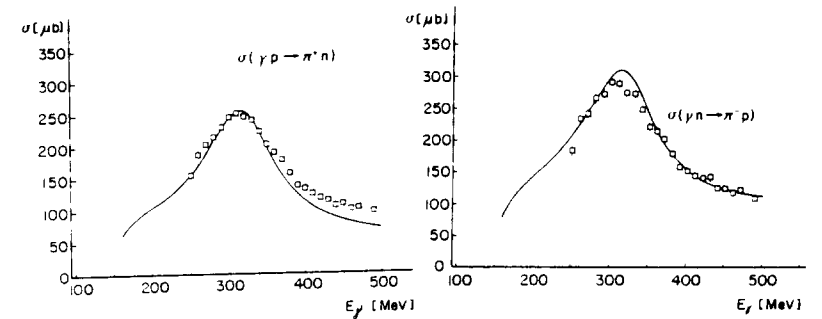

fig. 2 Cross sections for the $\gamma p \to \pi^+ n$ and $\gamma n \to \pi^- p$ reactions as a function of the photon energy. Experiment from [5].

3   The $\gamma N \to \pi\pi$ reaction.

Much experimental information is piling up on this reaction. To the old data in the late 60's [6, 7] one is adding new data from Mainz with an improved precission [8, 9]. The theoretical work has followed a similar trend. There is an early model which reproduces qualitatively the basic features of the reaction [10], but recently the model has been enlarged to include extra terms which prove to be important [8, 11]. The most complete model is the one of ref. [11] which contains 67 Feynman diagrams and accounts for N, $\Delta(1232)$, $N^*(1440)$, $N^*(1520)$ baryon intermediate states plus terms in which the two final pions couple strongly to the ρ-meson. Schematically the diagrams are classified according to the scheme of fig. 3.
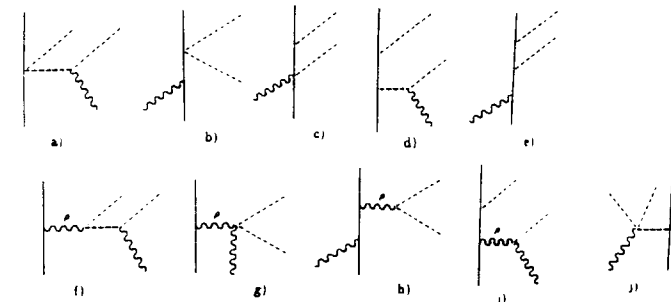

4

5

Fig. 3. Classification of the Feynman diagrams for $\gamma N \to \pi\pi N$ into one point, two point and three point diagrams.

The reader is addressed to ref. [11] for details but here I would like to stress one of the most interesting findings of the model. The dominant term in the $\gamma p \to \pi^+\pi^- p$ reaction is the one shown in fig. 4a, which involves the $\gamma N \Delta\pi$ Kroll Ruderman term and the decay of the Δ into $N\pi$

fig. 4 a) Dominant term in the $\gamma p \to \pi^+\pi^- p$ reaction. b) term involving the $N^*(1520)$ resonance and its decay into the $\Delta\pi$ system, which interferes with a) producing the peak of the cross section.

The term in fig. 4b involves the intermediate $N^*(1520)$ resonance, decaying into $\Delta\pi$ plus the Δ decaying into πN. This term is essential to reproduce the peak of the cross section which we see in fig 5.
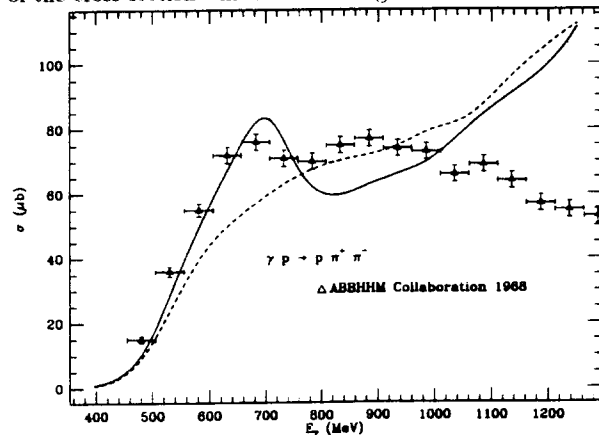
fig. 5: Total $\gamma p \to \pi^+\pi^- p$ cross section. Dashed line: the model of [11] omitting the $N^*(1520)$ terms; continuous line: complete model.

Contrary to simple intuition, the experimental peak of fig. 5 is not associated with the Δ excitation in the dominant term of fig. 4a. The reason is that there is no particular γ energy which places the Δ on shell since the π^- already

takes away some of the photon energy and its energy is distributed according to phase space. Consequently, the model, omitting the $N^*(1520)$ terms has a monotonous growth with energy, as seen in fig. 5, and the qualitative features of the cross section are missed. The term of fig. 4b happens to have the same spin structure as the term in fig. 4a, and then there is a constructive interference before the on shell energy of the $N^*(1520)$ is reached in the intermediate state and a destructive interference after. In this way the peak of the solid line shown in fig. 5 is reached as an interference phenomenon. The strength of the $N^* \to \Delta\pi$ coupling is taken from experiment. The sign is taken so as to have the best agreement with experiment in fig. 5 (the opposite sign produces unacceptable results) and it agrees (also the strength) with results for that coupling obtained in the constituent quark model for baryons [12].

The model of [11] also reproduces quite well mass distributions for the $(p\pi^-), (p\pi^+)$ and $(\pi^+\pi^-)$ systems. The discrepancies of the model with experiment from $E_\gamma = 1000\ MeV$ on should be expected since at those energies many more resonances than those considered in [11] would play a role in the reaction. Work on the other isospin channels is in progress along the lines of model [11] and experiments are also coming [8, 9].

4 Photonuclear cross section. The many body approach.

The many body approach followed in [1] begins by looking at the behaviour of a photon in infinite nuclear matter. Through the interaction of the photon with the matter it acquires a selfenergy $\Pi(k)$, or equivalently the photon of momentum k feels an optical potential $V_{opt}(k)$ defined in terms of $\Pi(k)$ as $2kV_{opt}(k) \equiv \Pi(k)$. Now let us take the wave function of the photon which will have its time dependence modified by the effect of the extra potential.

Hence we have

$$\Psi_\gamma \sim e^{-ikt}e^{-iV_{opt}t}\ldots \sim e^{-iImV_{opt}t}\ldots$$

$$|\Psi_\gamma| \sim e^{2ImV_{opt}t}\ldots \equiv e^{-\Gamma t}\ldots \qquad (5)$$

where the latest result is obtained because the other terms with t dependence have modulus one. Hence we observe that the presence of the optical potential induces a depletion of the photon wave through the medium such that

$$-\frac{1}{N}\frac{dN}{dl} = -\frac{1}{N}\frac{dN}{dt} = \Gamma = -2ImV_{opt} = -\frac{1}{k}Im\Pi(k,\rho) \qquad (6)$$

where we have written Γ explicitly as a function of k and ρ, the density of the medium. Thus, $-Im\Pi/k$ is the probability of photon reaction per unit length. Multiplying this probability by dl and ds we obtain a contribution to a cross section. Next, in order to obtain σ_A in a finite nucleus one makes use of the

local density approximation. by substituting $\rho \to \rho(\vec{r})$ and by integrating over the whole nuclear volume one obtains the formula

$$\sigma_A = -\int d^3r \frac{1}{k} Im\Pi(k, \rho(\vec{r})) \qquad (7)$$

There is always an approximation involved in the use of the local density approximation. However, in the present case because the contribution to σ_A is a volume contribution, the local density approximating is an excellent tool and the results one obtains with eq. (7) are the same that one obtains if one convolutes the density with a certain range of the interaction [1].

This appreciacion results in an economical and accurate tool to evaluate photonuclear cross sections, since calculations in nuclear matter are much simpler than the equivalent ones in finite nuclei.

The next step consists in the evaluation of the photon selfenergy and we proceed in parts. By starting from the model for $\gamma N \to \pi N$, folding the diagrams with their complex conjugates and summing over the occupied states we obtain the set of 36 Feynman diagrams represented in fig. 6
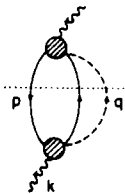

Fig. 6 Photon selfenergy diagram obtained by folding the $\gamma N \to \pi N$ amplitude. The circle indicates any of the terms of this amplitude from fig. 1.

The evaluation of $\Pi(k)$ for the diagramas of fig. 6 is easy. Assume for simplicity only one term, the Kroll Ruderman term, in the $\gamma p \to n \pi^+$ amplitude. We obtain then

$$-i\Pi_{p,n}(k) = \int \frac{d^4q}{(2\pi)^4} i\bar{U}_{p,n}(k-q) iD_0(q)(e\frac{f}{\mu}\sqrt{2}\frac{2M}{2M+k})^2 \qquad (8)$$

where $\bar{U}_{p,n}$ is the Lindhard function for ph excitation of fig. 6 of the (p,n) type and $D_0(q)$ the pion propagator. $Im\Pi(k)$ can be easily obtained using Cutkosky rules [13]. The imaginary part of Π is obtained when in the intermediate integrations the states cut by the dotted line in fig. 6 are placed on shell. In practical terms this is carried out by using the following useful rules (Cutkosky rules): Substitute

$$\Pi \to 2i Im\Pi$$

$$\bar{U}(q) \to 2i\theta(q^0)Im\bar{U}(q) \qquad (9)$$

$$D_0(q) \to 2i\theta(q^0)ImD_0(q)$$

By making this substitution and summing over the 6 terms of the $\gamma p \to \pi^+ n$ amplitude we obtain

$$Im\Pi(k)_{p,n} = \int \frac{d^3q}{(2\pi)^3} \theta(k^0 - \omega(q))Im\bar{U}_{p,n}(k-q)\frac{1}{2\omega(q)}\Sigma_n\Sigma_{sf}|T_{\gamma p \to \pi+n}|^2 \qquad (10)$$

By summing now also over the $(p,p),(n,p),(n,n)$ excitations one would obtain the whole photon selfenergy. It is instructive to see what has been accomplished with this step. For this purpose recall the limit when $\rho_p \to 0$

$$\theta(q^0)Im\bar{U}_{p,n}(q) = -\pi\rho_p\delta(q^0 - \vec{q}^2/2M) \qquad (11)$$

By means of this and the standard formulas for the cross section in terms of $|T|^2$, and using eq. (7) we obtain

$$\sigma_A = \sigma_{\gamma p}\int \rho_p(\vec{r})d^3r + \sigma_{\gamma n}\int \rho_n(\vec{r})d^3r$$

$$= \sigma_{\gamma p}Z + \sigma_{\gamma n}N \qquad (12)$$

with $\sigma_{\gamma p},\sigma_{\gamma n}$ the cross section for $\gamma p \to \pi N$ and $\gamma n \to \pi N$ respectively. This result is the impulse approximation. Eq. (11) neglects the effect of Pauli blocking and Fermi motion of the Lindhard function. It is thus clear that the use of eq. (10) improves over the impulse approximation precisely on these two points. However, it only takes into account the $\gamma N \to \pi N$ channel of the photonuclear reactions. The absorption channels are still missing.

The absorption channels can be easily obtained by allowing the pion in fig. 6 to excite a ph as shown in fig. 7. Then, when in the intermediate integrations the states cut by the dotted line in fig. 7 are placed on shell, this will give a contribution to $Im\Pi$ which is tied to the photon disappearing and producing a $2p2h$ excitation.
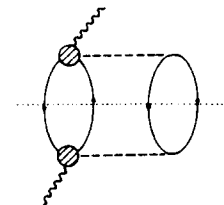
fig. 7. Photon selfenergy corresponding to photon absorption by a pair of nucleons.

The evaluation of the absorption diagrams is similar to the one we sketched for the (γ, π) channel, and now two Lindhard functions are involved in the evaluation of Π. There are many technical details which must be skipped here but can be followed from ref. [1], but we would like to mention that there are extra diagrams evaluated where the crossed circle happens in the second ph excitation, there are some symmetric terms which carry a symmetry factor $\frac{1}{2}$, and long range as well as short range correlation corrections are implemented into the scheme.

Around the region of excitation of the Δ resonance, the dominant contribution comes from the diagram of fig. 8
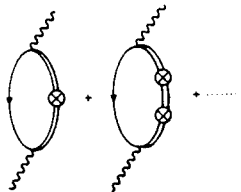

fig. 8. Δh excitation contribution to the photon selfenergy. The crossed circle indicates the Δ selfenergy insertion.

One finds there that

$$\Pi_\Delta(k) = (\frac{f_\gamma}{\mu})^2 \frac{4}{9}\vec{k}_{CM}^2 \frac{1}{\sqrt{s_\Delta} - M_\Delta + \frac{i\tilde{\Gamma}(k)}{2} - \Sigma_\Delta(k)} \rho \qquad (13)$$

where $\tilde{\Gamma}(k)$ is the free Δ width corrected by Pauli blocking and $\Sigma_\Delta(k)$ is the Δ selfenergy. The model for the Δ selfenergy is taken from ref. [14] and has both a real and an imaginary part. The latter part accounts for $\Delta N \to NN$ or $\Delta NN \to NN$ channels, which when implemented in eq. (13) lead to mechanisms of direct photon absorption by two or three nucleons. The important thing to keep in mind is the fact that

$$\frac{\tilde{\Gamma}(k)}{2} - Im\Sigma_\Delta(k) = \frac{\Gamma_{eff}}{2} > \frac{\Gamma(k)}{2} \qquad (14)$$

where $\Gamma(k)$ is the free Δ width. Hence, when we are close to the Δ pole, $\sqrt{s} - M_\Delta - Re\Sigma_\Delta(k) \simeq 0$, the Δh propagator in eq. (13) behaves as $2/i\Gamma_{eff}$ and are find that

$$|Im\Pi_\Delta| \sim \frac{1}{\Gamma_{eff}} < \frac{1}{\Gamma} \qquad (15)$$

and consequently the photonuclear cross section per nucleon with the renormalized Δ becomes smaller than the free γN cross section.

This feature is clearly visible in the experimental and theoretical cross sections which we show in figs. 9 and 10.

fig. 9. σ_γ/A for ^{12}C and ^{16}O. The experimental data are from [15] and [16] respectively.

fig. 10 σ_γ/A for ^{208}Pb. The dashed line shows the impulse approximation $(Z\sigma_{\gamma p} + N\sigma_{\gamma n})/A$. The dotted line shows the results for direct photon absorption . The experimental data are from: full circles [17], open circles [15].

In figs. 9 and 10 we also show the cross section corresponding to direct γ absorption. As we described before, the method we use traces back the γ cross section to the imaginary part of the γ selfenergy, and by looking at the different sources of imaginary part we can associate them to particular

fig. 7. Photon selfenergy corresponding to photon absorption by a pair of nucleons.

The evaluation of the absorption diagrams is similar to the one we sketched for the (γ, π) channel, and now two Lindhard functions are involved in the evaluation of Π. There are many technical details which must be skipped here but can be followed from ref. [1], but we would like to mention that there are extra diagrams evaluated where the crossed circle happens in the second ph excitation, there are some symmetric terms which carry a symmetry factor $\frac{1}{2}$, and long range as well as short range correlation corrections are implemented into the scheme.

Around the region of excitation of the Δ resonance, the dominant contribution comes from the diagram of fig. 8

fig. 8. Δh excitation contribution to the photon selfenergy. The crossed circle indicates the Δ selfenergy insertion.

One finds there that

$$\Pi_\Delta(k) = (\frac{f_\gamma}{\mu})^2 \frac{4}{9} \vec{k}_{CM}^2 \frac{1}{\sqrt{s_\Delta} - M_\Delta + \frac{i\tilde{\Gamma}(k)}{2} - \Sigma_\Delta(k)} \rho \qquad (13)$$

where $\tilde{\Gamma}(k)$ is the free Δ width corrected by Pauli blocking and $\Sigma_\Delta(k)$ is the Δ selfenergy. The model for the Δ selfenergy is taken from ref. [14] and has both a real and an imaginary part. The latter part accounts for $\Delta N \to NN$ or $\Delta NN \to NN$ channels, which when implemented in eq. (13) lead to mechanisms of direct photon absorption by two or three nucleons. The important thing to keep in mind is the fact that

$$\frac{\tilde{\Gamma}(k)}{2} - Im\Sigma_\Delta(k) = \frac{\Gamma_{eff}}{2} > \frac{\Gamma(k)}{2} \qquad (14)$$

where $\Gamma(k)$ is the free Δ width. Hence, when we are close to the Δ pole, $\sqrt{s} - M_\Delta - Re\Sigma_\Delta(k) \simeq 0$, the Δh propagator in eq. (13) behaves as $2/i\Gamma_{eff}$ and are find that

$$|Im\Pi_\Delta| \sim \frac{1}{\Gamma_{eff}} < \frac{1}{\Gamma} \qquad (15)$$

and consequently the photonuclear cross section per nucleon with the renormalized Δ becomes smaller than the free γN cross section.

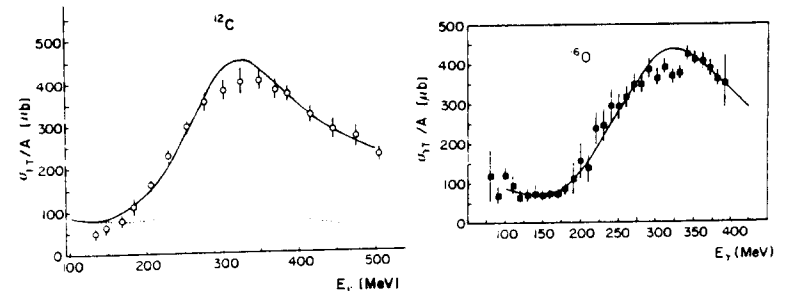This feature is clearly visible in the experimental and theoretical cross sections which we show in figs. 9 and 10.

fig. 9. σ_γ/A for ^{12}C and ^{16}O. The experimental data are from [15] and [16] respectively.
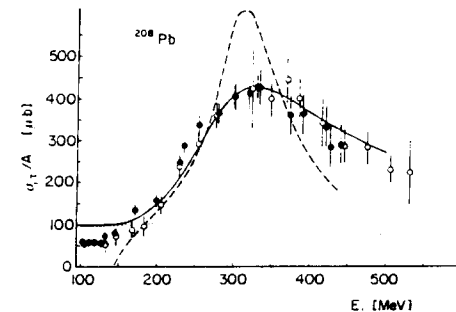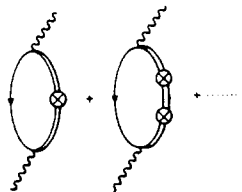

fig. 10 σ_p/A for ^{208}Pb. The dashed line shows the impulse approximation $(Z\sigma_{\gamma p} + N\sigma_{\gamma n})/A$. The dotted line shows the results for direct photon absorption . The experimental data are from: full circles [17], open circles [15].

In figs. 9 and 10 we also show the cross section corresponding to direct γ absorption. As we described before, the method we use traces back the γ cross section to the imaginary part of the γ selfenergy, and by looking at the different sources of imaginary part we can associate them to particular

channels like (γ, π) or γ absorption (see figs. 6 and 7). But we must be cautious in the interpretation. Eq. (7) gives a contribution to σ_A from each element of volume d^3r, and in each of these elements of volume we made the classification into (γ, π) or γ absorption. We are not saying anything about the fate of the particles emitted, nucleons or pions, in their may out of the nucleus, but are making a semiclassical assumption and this is that the final state interaction of these particles will not change the cross section, it will only redistribute its strength in different channels. This means that in some events that originally were of the (γ, π) type, the pion will be absorbed in its way out and show up as γ absorption, in the sense that only nucleons and no pions will be detected. We shall, thus, make a difference between this way of absorbing photons, which we call indirect photon absorption, and the direct one where originally no real pions were produced and the photon was directly absorbed.

The agreement with the data in figs. 9 and 10 is quite good. It is quite remarkable to see that even the small differences between σ_A/A for ^{12}C and ^{208}Pb that one obtains in the calculation have found experimental support in recent, very precise, measurements [18].

The assumption of the cross section not being modified by final state interaction is accurate for relatively energetic pions or nucleons (100 MeV or 50 MeV kinetic energies respectively). For low energy pions is should be less accurate, but then, for phase space reasons, the contribution to σ_A is small since the cross section is dominated by γ absorption. Thus, for photons with $\omega_\gamma \simeq 100$ MeV on, the assumption leads to accurate total cross sections.

It is also interesting to note that although σ_A/A is nearly constant for nuclei, up to the small differences apreciated in [18], the direct γ absorption per nucleon is not so constant for different nuclei, as comparison of the results for ^{12}C and ^{208}Pb in figs. 9 and 10 shows.

It is also interesting to note that for γ energies below $\omega_\gamma = 150$ MeV, the absorption cross section is dominated by the Kroll Ruderman and pion pole terms (see fig. 1). These terms are only relevant for charged pions and this implies γ absorption by pn pairs, something corroborated experimentally and which has been the foundation of the quasideuteron model for γ absorption [19]. Here we find a microscopical picture for γ absorption which supports some of the features of the quasideuteron (empirical) model and extends it to higher energies where the presence of the Δ allows for γ absorption or pp, pn or nn pairs.

We should also note that by starting from the $\gamma N \rightarrow \pi\pi N$ amplitude, taking the dominant Kroll Ruderman Δ term and folding the amplitude like in the case of the $\gamma N \rightarrow \pi N$ amplitude, we find terms contributing to the γ selfenergy like those depicted in fig. 11 and which contribute about 20% to the γ total cross section at energies around 450 MeV.
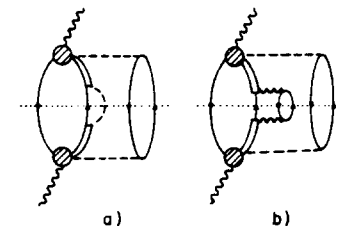

fig. 11: Channels tied to the $\gamma N \rightarrow \pi\pi N$ amplitude. a) corresponds to $2p h 1\pi$ excitation; b) corresponds to $3ph$ excitation.

5 Inclusive (γ, π) cross section.

In the former section we calculated σ_A and separated from it the cross section corresponding to direct photon absorption. The difference between σ_A and σ of direct absorption corresponds to events which originally were (γ, π), this is, where a real pion was produced in the first step. However, this pion is produced at a point $\vec{r}$ and before it goes out and can be detected it has to sort out many obstacles. Indeed, the pion can scatter with nucleons in its way out of the nucleus changing direction and energy; it can also be absorbed by pairs or trios of nucleons and then it will not be detected, instead, some nucleons will be ejected from the nucleus and the event will correspond to γ absorption of the indirect type as we discussed.

In order to be able to get cross sections for (γ, π) which can be compared to experiment it is imperative to follow the evolution of the pions in the nucleus once they are produced. This is done in ref. [20] and we outline the procedure here.

In ref. [21] a thorough study of all the inclusive pionic reactions was done: quasielastic, single charge exchange, double charge exchange and absorption. The procedure used there was the following: through a many body theory similar to the one described here for photons, one evaluated the pion reaction probabilities per unit length for the different reaction channels. Then all this information was used in a Monte Carlo simulation procedure which, according to the calculated probabilities, decides the different steps that the pion follows in its attempt to leave the nucleus. The procedure proves to be very accurate and effective to calculate all the pion reaction channels for pions above $E_\pi = 100$ MeV [21]. One could even prove there that the results for the total reaction cross section calculated with the Monte Carlo procedure were in very good agreement ($\sim 5\%$ differences) with the full quantum mechanical calculation of this channel. This latter calculation was done by solving the Klein Gordon equation for the pion with the pion nucleus optical potential

calculated microscopically, evaluating then the total cross section from the forward scattering amplitude using the optical theorem, and subtracting the integrated elastic cross section.

The same procedure used in [21] was followed in ref. [20] to follow the fate of the pion produced in a (γ, π) step. Some of the pions are absorbed and then we get indirect photon absorption. Others scatter quasielastically with nucleons and eventually change their charge. The simulation then tells us in which direction, and with which charge and energy the pions come out, allowing direct comparison with experiment.

The agreement of the results of [20] with experiment is rather good in all charge pion channels, double differential cross sections, angular or energy distributions and for different nuclei. We show in fig. 12 results for $(\gamma, \pi^\pm)$ for different nuclei, where one observes that, once the proper cuts considered in the experiment are taken into the account, the agreement of theory and experiment is rather good.
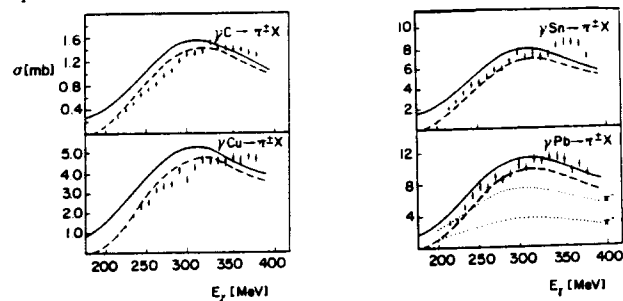

fig. 12. Integrated cross sections for $(\gamma, \pi^\pm)$ for several nuclei as a function of the photon energy. Continuous line: integrated cross section; dashed line: calculation omitting the pions with $T_\pi < 40\ MeV$ to compare with experiment. Experimental data from ref. [22]. Dotted line: theoretical contribution from (γ, π^+) and (γ, π^-), both of them without pion threshold.

Since the (γ, π) cross sections come out fine from our calculations and so do the total cross sections, then we are also making accurate predictions for the total absorption cross section. However, our calculations allow us to distinguish between direct and indirect photon absorption. In fig. 13 we show the direct absorption, total absorption and total cross sections per nucleon for photons interacting with ^{12}C and ^{208}Pb.

It is very interesting to note that the amount of indirect photon absorption per nucleon in ^{208}Pb is about three times larger than in ^{12}C. The result is intuitive because in a heavy nucleus the pions have less chances to leave the nucleus without being absorbed. However, one should not overlook this finding which shows that the amount of γ indirect absorption in nuclei provides

more information on pion absorption than the experiments of pion absorption with real pions. The reason is that for pions close to the resonance the pion absorption probability per unit length is so big that all pions which come into the absorption probability cross section of the nucleus get absorbed and the cross section the geometrical cross section goes roughly as πR^2 (R, nuclear radius). In this case this cross section is rather insensitive to the intrinsic absorption probability per unit length. Indeed, if we increase this probability in a calculation, the pions are absorbed sooner but are absorbed anyway. In simple words, a black disk can not become blacker. On the other hand the probability that a pion created in a point leaves the nucleus is proportional to

$$e^{-\int P_{abs}\, dl} \tag{16}$$

and this exponential is very sensitive to P_{abs}. The discussion above can be summarized in simple words by saying that the magnitude of indirect photon absorption in nuclei can provide more information about pion absorption probabilities than the pion absorption cross sections obtained from the scattering of real pions on nuclei. In view of this finding it looks quite useful to invest efforts into the experimental separation of the two sources of photon absorption throughout the periodic table. The techniques to be used would ressemble those used in the separation of genuine three nucleon pion absorption from quasielastic steps followed by two body absorption [23].
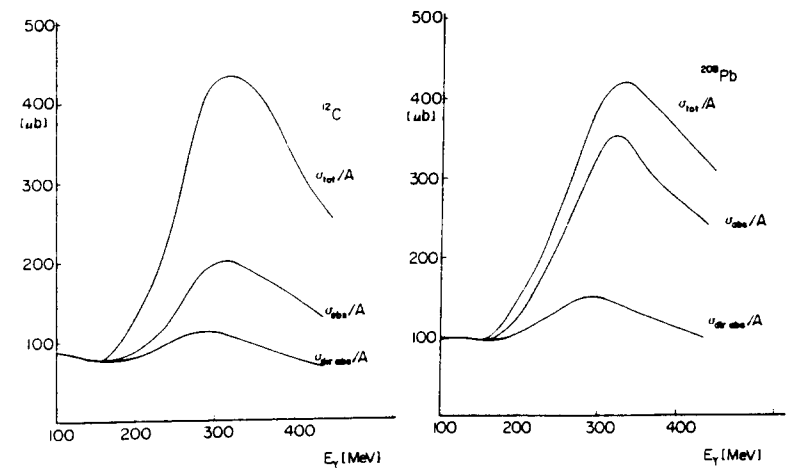

fig. 13. a) Photonuclear cross section for ^{12}C. Upper curve: total photonuclear cross section; middle curve: total absorbtion; lower curve: direct photon absorption. b) Same for ^{208}Pb.

6 Inclusive $(\gamma, N), (\gamma, NN), (\gamma, \pi N) \ldots$ reactions.

The detailed work on these channels has been done in ref. [24]. The work is a natural continuation of the study in the (γ, π) channel in ref. [20]. Here, in addition to the final state interaction of the pions, one also pays attention to the final state interaction of the nucleons. The nucleons coming from (γ, π), γ absorption or pion absorption can collide with other nucleons changing energy, direction and charge. A calculation which attempts to compare with experiment necessarily has to address this problem.

The key ingredient in the final state interaction of the nucleons is the nucleon mean free path through matter, which is known to be larger than the semiclassical estimate, $\lambda^{-1} = \sigma_{NN}\rho$ [25]. A more suited magnitude than the mean free path is the imaginary part of the N-nucleus optical potential. The analysis of [24] uses a semiphenomenological model, developed in [26], which reproduces fairly well the microscopic results of ref. [27] obtained with a substantially larger computational time.

The sources of nucleons in photonuclear reactions are varied:

i) direct γ absorption

ii) (γ, π) knock out

iii) (π, π') knock-out

iv) π absorption

v) NN collisions

In [24] once again a Monte Carlo computer simulation was performed to account for final state interaction of pions and nucleons. It was also proved in [24] that the reaction cross sections for N-nucleus scattering calculated with the simulation or quantum mechanically were also very similar, with about $5-8\%$ differences for different nuclei and nucleons with kinetic energy bigger than $40\ MeV$. This observation gives one confidence in the Monte Carlo simulation to investigate the different reaction channels, which would be technically forbidden otherwise.

Less ambitious studies of NN emission, with the consideration of direct photon absorption as the only source, have been carried out elsewhere [28, 29].

The results of [24] for the (γ, N) channel agree only semiquantitatively with experiment. The agreement is good in some nuclei while in other nuclei and certain energies there can be a disagreement of about a factor of two.

In the (γ, NN) and $(\gamma, \pi N)$ channels there is much work going on experimentally [30] and comparisons are being made with the predictions of ref. [24]. Work is still in progress but we expect to be able to extract much information about the dynamics of basic processes like pion absorption, photon direct absorption, nucleon mean free path in nuclei, isospin dependence of basic mechanisms, etc.

7 Conclusions.

From the discussions above one can draw the following conclusions, which I classify into some pertaining to the theoretical side and others to the experimental side.

A) Theoretical side:

i) A microscopic many body picture for the photonuclear processs is possible combining elements of pion physics with photonuclear dynamics.

ii) All inclusive channels $(\gamma, \pi), (\gamma, N), (\gamma, 2N), (\gamma, \pi N)$, etc., can be addressed simultaneously.

iii) The γ absorption cross section depends strongly on A and has two sources:

a) Direct absorption.

b) Indirect absorption ((γ, π) followed by π absorption).

In heavy nuclei the indirect absorption dominates the absorption cross section. The indirect absorption cross section goes roughly as A^α with $\alpha > 1$ (in π absorption $\alpha \simeq 2/3$). The study of indirect photon absorption will teach us much about pion absorption in nuclei.

B) Experimental side:

i) Work advisable to separate $(\gamma, pp), (\gamma, pn), (\gamma, nn)$ as a function of the energy to pin down the basic dynamics.

ii) Work necessary to disentangle direct from indirect photon absorption to avoid misleading messages about γ absorption.

iii) Information from pion physics is essential to interprete correctly the results.

iv) The amount of experimental information in coincidence experiments is so large that real efforts are needed to classify it into a practical and useful way, which allows one to learn about the basic dynamics of the physical processes. In view of the fairly large amount of channels present in these reactions, the extraction of the basic dynamics is not easy without a strong theoretical guidance. It is most available that the experimental analysis goes side by side with theoretical calculations, as complete as possible, in order to establish solid facts about the basic dynamics of the processes by learning both from the agreement and disagreament of the predictions with the data. The fact that many experimental groups have reached this conclusion [30] is an encouraging sign that much progress is ahead.

References

[1] R. C. Carrasco and E. Oset, Nucl. Phys. A536(1992)445.

[2] I. Blomqvist and J.M. Laget, Nucl. Phys. A280(1977)405.

[3] S. Fubini, G. Furlan and C. Rossetti, Nuovo Cim. 40 (1965)1171.

[4] M. G. Olson, Nucl. Phys. B78(1974)55.

[5] T. Fujii et al., Nucl. Phys. B120(1977)395.

[6] Aacher-Berlin-Bonn-Hamburg-Heidelberg-München collaboration, Phys. Rev. 175(1968)1669.

[7] G. Gianella et al., Nuovo Cimento 63A(1969)892.

[8] L. Murphy, PhD Thesis, Saclay, 1993.

[9] H. Ströher et al., invited talk at the Int. Conf. on Mesons in nuclei, Dubna, May 1994.

[10] L. Lüke and P. Söding, Springer tracts in modern physics, vol. 59 (Springer, Berlin, 1971) p. 39.

[11] J. A. Gómez Tejedor and E. Oset, Nucl. Phys. A571(1994)667.

[12] F. Cano, Tesina de Licenciatura, Universidad de Valencia, 1994.

[13] C. Itzykson and J.B. Zuber, Quantum Field Theory (Mc Graw Hill, New York, 1980).

[14] E. Oset and L.L. Salcedo, Nucl. Phys. A468(1987)631.

[15] L. Guedira, PhD Thesis, University of Paris Sud, 1984.

[16] J. Ahrens et al., Nucl. Phys. A490(1988)655.

[17] P. Carlos et al., Nucl. Phys. A431(1984)573.

[18] N. Bianchi, private communication.

[19] J. S. Levinger, Phys. Rev. 84(1951)43.

[20] R. C. Carrasco, E. Oset and L.L. Salcedo, Nucl. Phys. A541(1992)585.

[21] L.L. Salcedo, E. Oset, M.J. Vicente-Vacas and C. García-Recio, Nucl. Phys. A484(1988)557.

[22] H. Rost, PhD Thesis, Universität Bonn, 1980.

[23] H. Weyer, in the Int. Workshop on pions in nuclei, Peniscola, June 1991, E. Oset et al. Edts., World Scientific, pag. 441.

[24] R. C. Carrasco, M.J. Vicente-Vacas and E. Oset, Nucl. Phys. A570(1994)701.

[25] D. F. Geesaman et al., Phys. Rev. Lett. 63(1989)734.

[26] P. Fernández de Córdoba and E. Oset, Phys. Rev. C46(1992)1697.

[27] S. Fantoni, B. L. Friman and V. R. Pandharipande, Nucl. Phys. A399(1983)51; S. Fantoni and V. R. Pandharipande, Nucl. Phys. A427(1984)473.

[28] C. Giusti, F. D. Pacati and M. Radici, Nucl. Phys. A546(1992)607.

[29] J. Ryckebush, M. Vanderhaeghen, L. Machenil and M. Waroquier, Nucl. Phys. A568(1994)828.

[30] N. Rodning et al.; P. Grabmayer et al.; A. Sandorfi et al.; M. Ling et al., in preparation.